
# The development of a metallurgical flowsheet to treat tails

by J.R. Walklate* and H. Jeram†


## Synopsis

**The ilmenite, rutile and zircon processes of the Mineral Separation Plant generate tailing streams, which still contain valuable mineral. This is due to a combination of factors, which include separator equipment efficiency, particle size effects and inefficient operating practices (equipment overloading, blockage, etc.). Recent developments by metallurgical equipment suppliers have led to increased mineral separator performance enabling recovery of previously lost valuable mineral.**

**Mineralogical studies were conducted using QEM*SEM and MLA techniques to identify and quantify gangue mineral species and determine mineral association. Laboratory and pilot-scale test work was then conducted to develop suitable process flowsheets for the recovery of ilmenite, rutile and zircon from current and stockpiled tailings.**


## Introduction

Richards Bay Minerals (RBM) operates four mining plants producing sufficient heavy mineral concentrates (HMC) to satisfy the requirements of the smelting operation. The heavy mineral concentrate is screened and then separated on wet high intensity magnetic separators to recover ilmenite. The non-magnetic fraction is subjected to gravity separation on spirals to produce a rutile/zircon rich concentrate. The concentrate is dried and then separated on electrostatic and magnetic separators to produce saleable rutile and zircon products.

The various tailing streams produced contain valuable minerals not recovered by the process. These tails are combined and returned to the mining plant where they are stockpiled for future retreatment.

## Mineralogy of the tailing streams

The tailings can be magnetically fractionated using a high intensity magnet and the resultant fractions analysed on an X-ray fluorescence spectrometer (XRF) to determine elemental abundance. This will determine the amount of magnetic and non-magnetic titanium, zirconium and iron species present. It will not, however, identify the species. In order to develop metallurgical circuits to recover valuable mineral, the physical and chemical properties of the mineral assemblage are required.

Mineralogical characterization was carried out using QEM*SEM (quantitative evaluation of materials by scanning electron microscopy) on total and magnetically fractionated tailings samples[1]. The modal mineral abundance in each of the tailings streams is shown in Figure 1, and the physical properties of the minerals present summarized in Table I. Each tailings stream contained varying proportions of ilmenite, rutile/leucoxene and zircon. Information on the elemental assays determined chemically and calculated from QEM*SEM data showed good agreement.

The Feed Prep tailings (FPT) sample contained abundant zircon (18%) in addition to rutile/leucoxene (13%) and ilmenite (5%). Quartz and feldspar dominated the silicates and together with epidote, amphibole and garnet contributed to more than 50% of the sample.

The Wet Zircon tailings (WZT) sample was dominated by zircon (53%) with approximately 10% rutile/leucoxene and less than 1% ilmenite. Monazite was the most common phosphorus-bearing mineral present in the sample (3%) with epidote and amphibole the most common silicates.

The Scavenger tailings (ST) sample contained 34% ilmenite, 10% zircon and 7% rutile/leucoxene with epidote, amphibole and garnet making up 33% of the sample.


* *Richards Bay Minerals.*

† *Hatch Associated Ltd*


 *SA ISSN 0038–223X/3.00 + 0.00. This paper was first published at the SAIMM Conference,* Heavy Minerals, *10–14 September 2007*

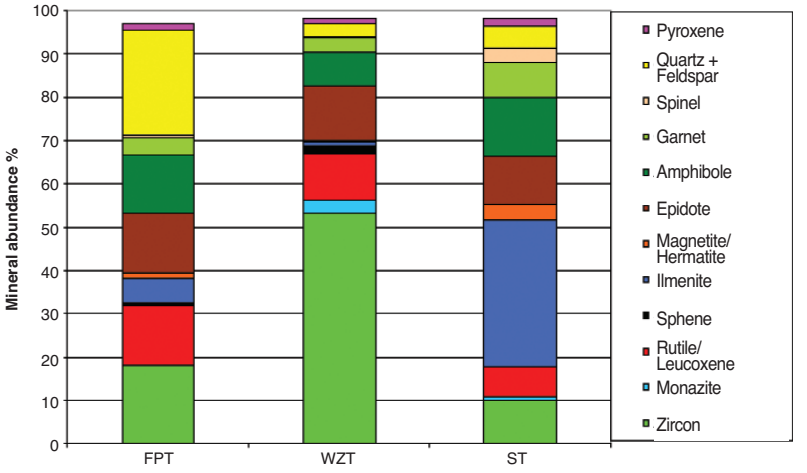


**Figure 1—Mineral abundance**

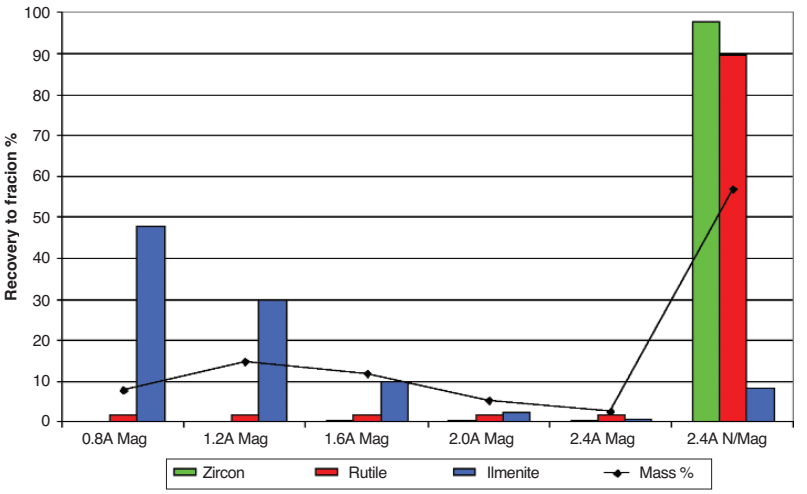


**Figure 2—Ilmenite, rutile and zircon recovery per magnetic fraction (FPT sample)**

The deportment of each mineral of interest (ilmenite, rutile and zircon) across the magnetic fractions was determined for each tails stream. The recovery of gangue minerals, which contribute significantly in terms of their abundance or as a carrier of penalty elements such as phosphorus, was also determined. This data is presented in Figures 2 and 3 for sample FPT.

For the FPT sample more than 89% of the rutile and zircon reported to the non-magnetic fraction. Ilmenite showed a variable magnetic response with 92% accumulated across the magnetic fractions. The recovery of silicate minerals indicated that epidote, amphibole and garnet also exhibited a variable magnetic response, whereas quartz was non-magnetic.

In the WZT sample more than 90% of the rutile and zircon reported to the non-magnetic fraction, with epidote, amphibole, garnet and monazite showing a variable magnetic response. For the ST sample nearly 90% of the ilmenite was recovered to the first magnetic fraction.

Significant association was found between ilmenite and rutile, which contributed to the misreporting of these minerals to the non-magnetic and magnetic fractions respec-

*Table I*

**Mineral properties[2]**

| Mineral | Specific gravity | Magnetic response | Electrostatic response |
|---|---|---|---|
| Zircon | 4.7 | Non-magnetic | Non-conductor |
| Monazite | 5.3 | Paramagnetic | Non-conductor |
| Rutile | 4.2 | Non-magnetic | Conductor |
| Leucoxene | 3.9 | Para/non-magnetic | Conductor |
| Sphene | 3.4 | Non-magnetic | Non-conductor |
| Ilmenite | 4.7 | Paramagnetic | Conductor |
| Magnetite | 5.2 | Ferromagnetic | Conductor |
| Haematite | 5.2 | Paramagnetic | Conductor |
| Epidote | 3.4 | Paramagnetic | Non-conductor |
| Amphibole | 3.2 | Paramagnetic | Non-conductor |
| Garnet | 3.9 | Para/non-magnetic | Non-Conductor |
| Spinel | 3.6 | Non/paramagnetic | Conductor |
| Quartz | 2.7 | Non-magnetic | Non-conductor |
| Pyroxene | 3.4 | Para / non-magnetic | Non-conductor |

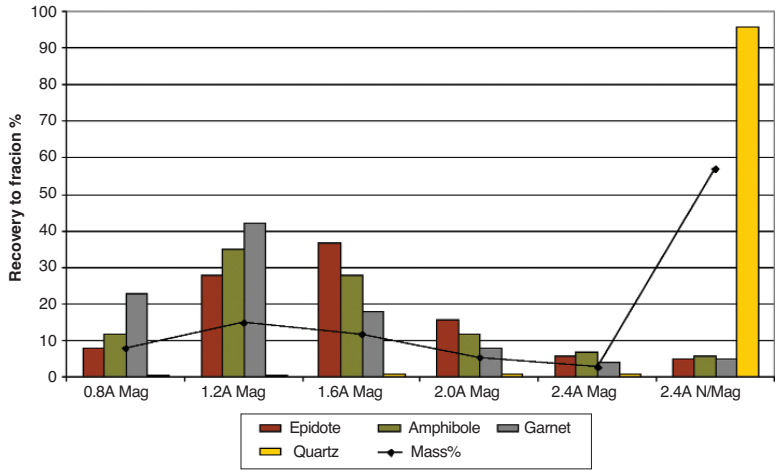


**Figure 3—Silicate recovery per magnetic fraction (FPT sample)**

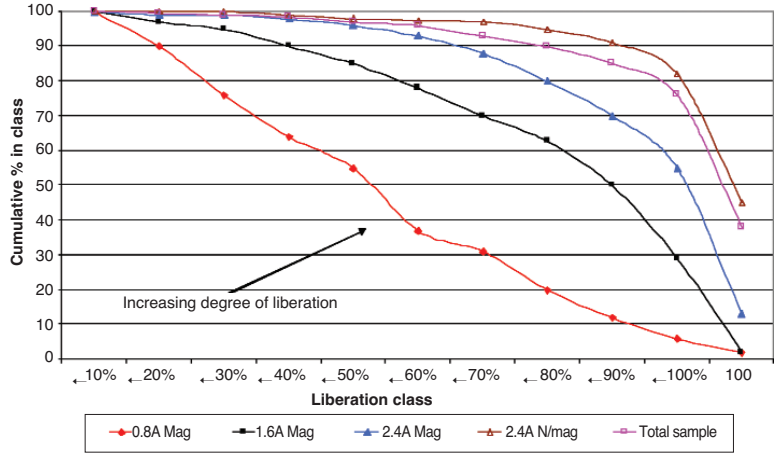


**Figure 4—Liberation characteristics—rutile in FPT sample**

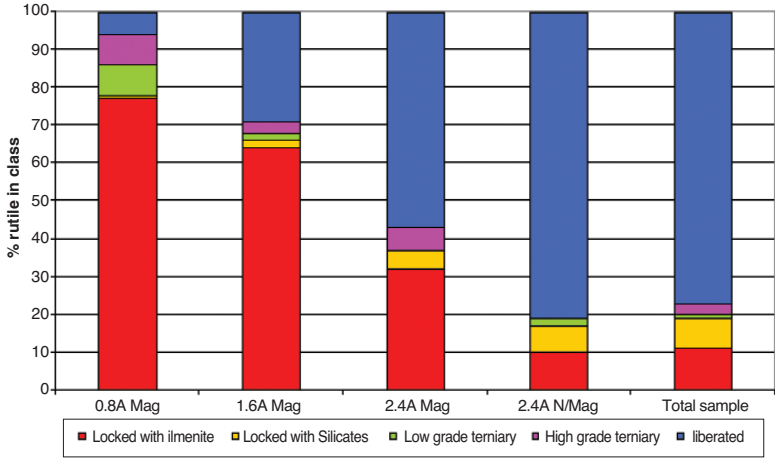


**Figure 5—Rutile locking characteristics (FPT sample)**

tively. An example of the liberation characteristics of rutile in the FPT sample is shown in Figure 4 and illustrates the variation in liberation across the magnetic fractions. Zircon was found to be highly liberated in all the tailings samples analysed.

The locking of ilmenite and rutile with other minerals was investigated, and an example for rutile is shown in Figure 5. A strong association is seen between the two minerals with significant proportions of non-liberated (<90%) rutile in binaries with ilmenite.

## Physical properties of the tailings streams

### *Particle size distribution*

Size analysis was conducted on individual tailings streams and on a combined tailings stream. The fractional and cumulative percentage size distributions for the individual tailings streams are presented in Figure 6 and the combined tailings stream in Figure 7. The FPT stream is significantly courser than the WZT and ST streams with a $d_{50}$ of approximately 170 microns compared to 130 to 140 micron.

The size fractions of the combined tailings were analysed for valuable and gangue minerals. The magnetic other minerals were shown to be coarser than the valuable minerals, with quartz exhibiting a bimodal distribution. The specific gravity and size distribution of the magnetic other minerals indicate that gravity separation (spiral or shaking table) could be employed to reject these minerals from the tailings. Rejection of the fine quartz would, however, be more difficult.

### *Gravity separation response*

The capital cost of gravity separation equipment is generally lower than magnetic separation units and is usually the first stage (after trash screening) of a mineral separation circuit. The purpose of the gravity circuit will be to remove quartz and low density magnetic other minerals while maximizing recovery of the valuable minerals present.

Tailings samples were subjected to gravity separation on a Wilfley laboratory shaking table to determine the potential grade and recovery of the concentrate produced. Similar tests were conducted using a variety of gravity spirals. Performance curves of recovery and collection efficiency versus concentrate yield were developed for comparative purposes, and examples are given in Figures 8 and 9 for recovery and efficiency respectively.

The 'ideal separation' line for zircon and the 'nil separation' line have been included. The distance between the mineral recovery curve and the 'nil separation' line is a measure of the separation efficiency. The Wilfley table exhibited a poor recovery curve for NM $TiO_2$ and a fairly flat curve for zircon. Quartz rejection was also poor due to the presence of fine silica. Similar recovery curves were achieved using the spiral separator. Tests were conducted using a Floatex density separator to reject fine and light mineral species prior to spiral separation. The recovery of zircon and

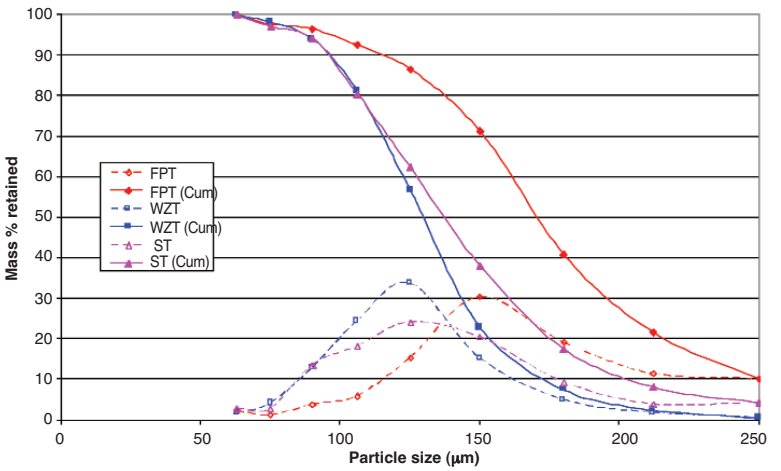


Figure 6—Particle size distribution (FPT, WZT, ST)

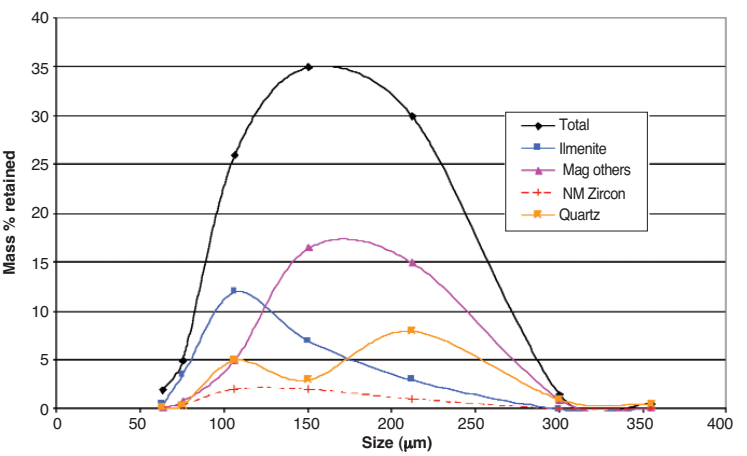


Figure 7—Particle size distribution (combined)

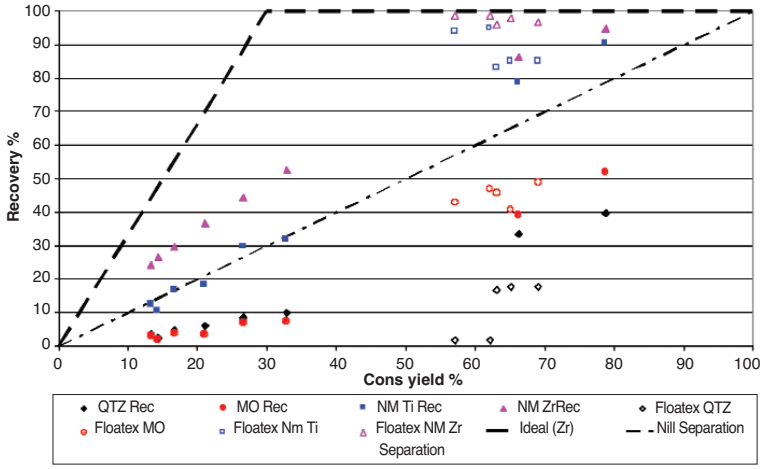


**Figure 8—Recovery vs. yield—Wilfley table**

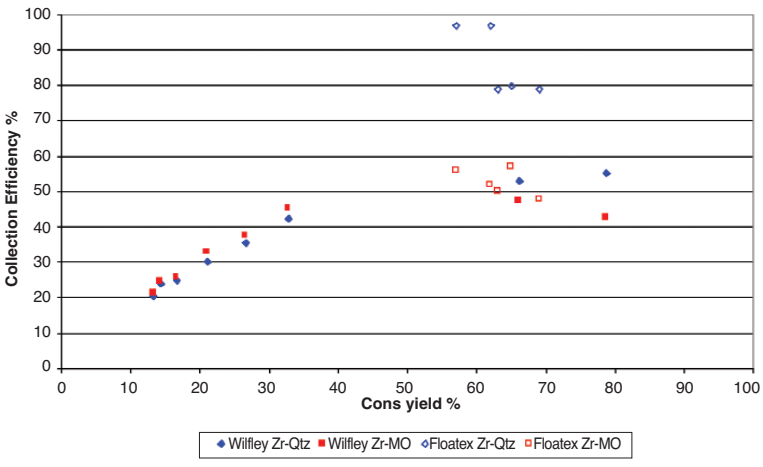


**Figure 9—Collection efficiency—Wilfley table and Floatex**

rejection of quartz was higher for the Floatex separator in comparison to the Wilfley table, with $TiO_2$ recovery and mag others' rejection being similar. This is clearly shown in Figure 9, which compares the collection efficiency of the two units. This is defined as the difference in recovery between the valuable species and the gangue species at a given concentrate yield[3]. The zircon-quartz efficiency was significantly higher for the Floatex while that of zircon-magnetic others was similar.

### *Magnetic separation response*

The purpose of the magnetic separation stage will be to maximize the rejection of magnetic gangue minerals from the spiral concentrate to produce an ilmenite-rich stream and a rutile/zircon-rich stream for further processing.

Samples of tailings were dried and separated using the laboratory induced roll magnet (IMR) and the rare-earth roll magnet (RER) to determine the potential for magnetic other removal. Excellent results were achieved and both magnet types exhibited similar performance curves for non-magnetic and magnetic others' recovery. 95% of the non-magnetics were recovered at a non-magnetic yield of 60%, with a corresponding rejection of 95% magnetic others.

Wet magnetic separations were carried out on the pilot plant wet high intensity magnetic separator (WHIMS) and the results compared to the dry magnet tests in Figure 10. The WHIMS appears to follow the dry magnet performance curves for both magnetic other and non-magnetic minerals. The mass yield to the non-magnetic product could not be reduced below 80%, however, and rejection of magnetic others was poor, as a result. As seen in Figure 10, the magnets should be operated at a non-magnetic product yield of approximately 60% for the most efficient separation. Although the efficiency of the WHIMS is below that of the dry magnets, the rejection of 20% of the mass prior to drying would be beneficial from a capital cost viewpoint (reduction in the size of the drier required and the number of dry circuit equipment).

### *Electrostatic separation response*

The purpose of the electrostatic separation stage is to produce a conductor fraction suitable for further processing in the rutile plant, a non-conductor fraction suitable for further processing in the zircon plant, and a reject middling fraction to negate a recycling load of 'difficult' material between the dry mill and the tailings plant.

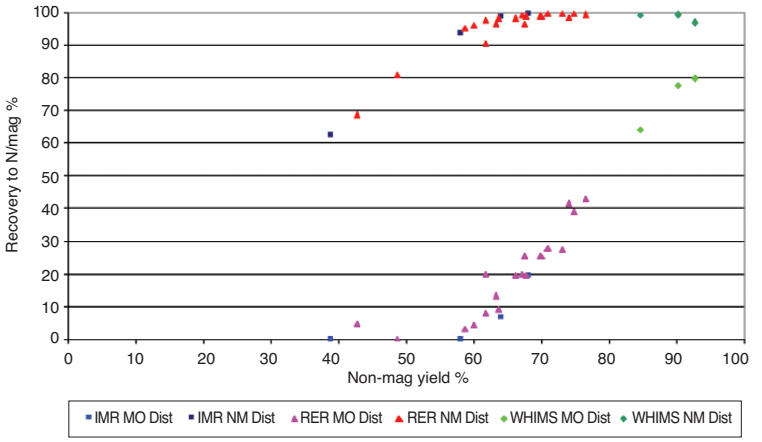


**Figure 10—Magnet performance curves**

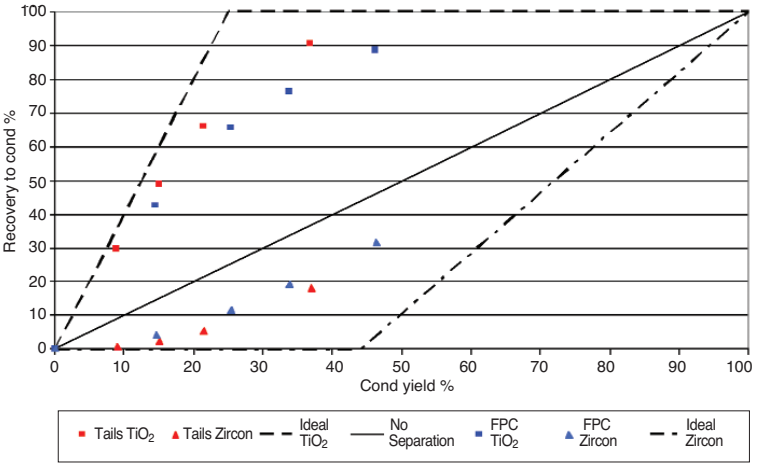


**Figure 11—HTR performance curves**

Samples of the non-magnetic product generated were dried, heated and passed over a high tension roll separator (HTR) to produce five fractions. Performance curves were generated from the data for NM $TiO_2$ and zircon recovery versus conductor yield (Figure 11). These curves were compared to those achieved on current dry mill feed (FPC) to determine whether adverse behavioural differences could be detected.

## Flowsheet development

Sample material for test work was sourced from stockpiled tailings near RBM. Current tailings from the plant were mixed with the stockpiled tailings for a representative feed to the proposed process. Approximately 5–8 tons were used for each run of test work in the pilot plant. Each unit operation of the proposed circuit was tested individually. Some tests were conducted on purely stockpiled material and others on a combination feed. The circuit included wet gravity and magnetic separation, followed by dry magnetic and electrostatic separation. Tests were conducted using this material in the pilot plant to confirm the mass balance for the proposed circuit and determine corresponding recoveries and grades achieved for the products. The gravity circuit included a Floatex density separator and spirals. The wet magnetic circuit included low intensity magnetic separation followed by high intensity magnetic separation to produce a magnetic product rich in ilmenite. The non-mags of the wet magnetic circuit was dried and treated over an electrostatic separator to produce conductor and non-conductor feed streams for dry magnetic separation. In Figure 12 the basic flow of material is represented to produce the magnetic ilmenite product and non-magnetic zircon and rutile products.

### *Gravity separation*

The Floatex density separator was used in the first stage of the gravity circuit primarily to reject fine quartz and reduce the amount of mag others in the feed to the wet magnetic circuit. The principle of Floatex operation is that a rising current of teeter water would enable the feed to classify itself during suspension so that the coarser and heavier particles will report to the underflow. Thus, fine quartz reports to the overflow due to its size and specific gravity. The Floatex was fed via the hopper and conveyor system of the pilot plant. The rejection of quartz and mag others needed to be maximized whilst achieving a good recovery of ilmenite, zircon and rutile. The teeter flow rate is dependent on the feed particle size distribution, density of the feed and the desired cut point for separation. Timed samples were taken of the underflow, overflow and feed to the unit at regular intervals. Larger sampling times were utilized to get a

# The development of a metallurgical flowsheet to treat tails

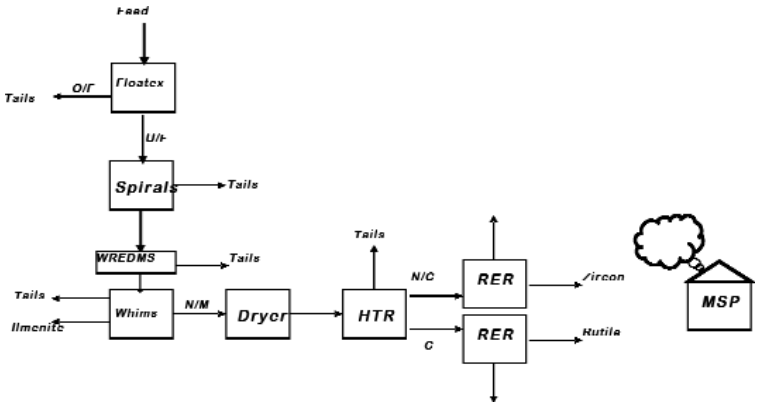


**Figure 12—Block diagram flowsheet**

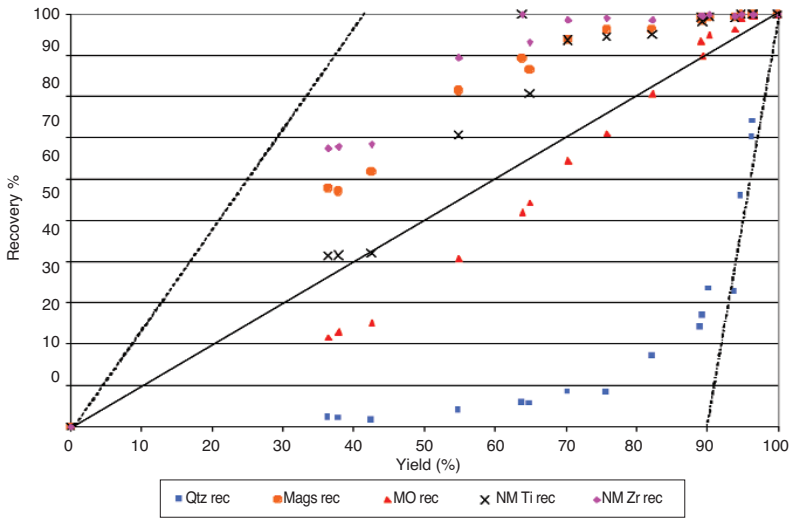


**Figure 13—Recovery vs. yield for primary spiral stage test work**

representative sample of both overflow and underflow rates over the full test period. Bulk samples were collected for further processing.

A mineral liberation analyser (MLA) uses a scanning electron microscope and an energy dispersive X-ray combined with quantitative mineralogical software to produce mineralogical information on mineral and material streams. MLA results are tabulated in Table II for the three streams entering and exiting the Floatex. It is noted that epidotes, pyroxenes and quartz form part of the major unwanted minerals. Heavier minerals increase in the underflow such as magnetite and the valuable minerals, while lighter minerals such as quartz, amphiboles and feldspar report to the overflow. The underflow from the Floatex was collected and subsequently fed to a primary stage of spirals. The three products of the spiral (concentrate, middlings and tailings) were collected in drums and timed samples were taken at regular intervals. The tailings were discarded. The middlings fractions were retreated on a second stage of spirals. The splitters were adjusted during operation by visual inspection. Two stages of spiral separation were used to enable maximum recovery of valuable minerals.

In Figure 13 the rejection of quartz and mag other minerals is maximized as it is furthest from the 'no separation' line. The NM $TiO_2$ and NM zircon recoveries

*Table II*

**Comparison of feed and product streams of Floatex density separator**

| Mineral | Floatex H/F % | Floatex O/F % | Floatex U/F % |
|---|---|---|---|
| Amphibole | 7.29 | 7.39 | 6.14 |
| Carb-calcite | 0.75 | 1.83 | 0.28 |
| Chromite | 0.97 | 0.14 | 2.02 |
| Clays | 4.41 | 2.19 | 5.00 |
| Epidote | 12.10 | 8.50 | 10.65 |
| Feldspar | 0.56 | 2.57 | 0.21 |
| Garnet | 5.24 | 1.16 | 5.09 |
| Haematite | 2.05 | 0.04 | 2.47 |
| Ilmenite | 13.45 | 0.60 | 16.24 |
| Ilmenite-alt | 1.27 | 0.25 | 1.68 |
| Kyanite & Silica | 0.05 | 0.01 | 0.13 |
| Leucoxene | 1.85 | 0.71 | 1.69 |
| Magnetite | 2.86 | 0.34 | 3.86 |
| Other | 0.34 | 0.14 | 0.39 |
| Phosphates | 0.89 | 0.32 | 1.12 |
| Pyroxene | 11.50 | 10.73 | 12.76 |
| Quartz | 13.03 | 60.43 | 2.76 |
| Rutile | 5.47 | 1.01 | 6.56 |
| Spinel | 0.19 | 0.01 | 0.46 |
| Staurolite | 0.67 | 0.04 | 0.75 |
| Titanite-sphene | 0.48 | 0.46 | 0.69 |
| Tourmaline | 0.14 | 0.26 | 0.11 |
| Zircon | 14.45 | 0.84 | 18.94 |
| Total | 100.00 | 100.00 | 100.00 |

follow close to the ideal separation envelope (dashed lines) as well. Similar recovery of minerals was noted for the secondary stage spiral retreatment of the primary stage middlings fraction. The primary and secondary stage spiral concentrates were dried for further magnetic separation tests in the pilot plant.

### *Wet magnetic separation*

The combined spiral concentrates were treated over a wet rare-earth drum magnet to reject highly magnetic material prior to WHIM separation. Tests were conducted on 50 to 100 kg of combined spiral concentrate samples at a time. A Reading WHIMS 8 pole unit in the pilot plant was utilized for all tests. The material was dry fed at a controlled rate and slurried with a predetermined volume of water prior to entering the WHIMS feed box. Tests were conducted at flow rates of 2.5 and 2.0 TPH per feed point on the pilot plant WHIMS unit. Improved separation was achieved at lower feed rates. It is known that as coil current is increased, the magnetic recovery is higher due to the rise in magnetic flux density; however, the entrainment of non magnetic and mag other minerals increases.

Two products were collected. The ilmenite was concentrated in the magnetic product. The products were dried and split for analysis. The magnetic product from the first stage of WHIMS was retreated at reduced amps. Further stages of retreatment were utilized to increase the grade of the ilmenite, within the specified $Cr_2O_3$ and CaO impurity levels for smelter feed.

The non-magnetic product from the first stage was treated at high amp setting to remove the maximum amount of magnetic mineral from the zircon and rutile rich product. This non-magnetic product was dried and split for dry circuit simulation tests.

### *Electrostatic separation*

Pilot tests were conducted on the dried non-magnetic product from the secondary WHIMS stage for stockpiled and mixed material on the Coronastat high tension roll separator and the Inprosys rare-earth roll magnet.

*Table III*

**HTR performance on rutile and zircon grade and recoveries from WHIMS non-mag product**

| | Yield % | $TiO_2$ | | Zircon | |
|---|---|---|---|---|---|
| | | Grade% | Recovery% | Grade% | Recovery% |
| Conductors | 14.3 | 61.9 | 50.5 | 9.3 | 2.2 |
| Non-conductors | 72.2 | 4.3 | 19.0 | 69.7 | 90.1 |

Sample sizes ranged from 3–5 kg for dry circuit simulations. The feed contained 14% $TiO_2$ and 56% zircon for this test. HTR work was conduced at approximately 95°C. The secondary WHIMS non-mags material was heated in the laboratory fluid bed dryer. The same dryer was used to reheat the mids for three-stage retreatment to the same temperature. The roll speed was set to 60 Hz on this particular unit. The voltage was set to 25 kV and fed at a rate of 2.0 TPH/m.

The mids fraction after the third stage made up 12.7% mass yield with 39.9% $TiO_2$ and 34.5% zircon grade.

Figure 14 is used to illustrate the typical variation in mass yield between conductors and non-conductors with a middlings retreat in the HT roll test work. As the mids fraction was treated in subsequent stages, the mass yield per stage decreases from 43.7% to 22.6% to 13.5% in the third stage. The non-conductor yield increases from 49.6% to 66.2% to 72.2% in the final stage. The products of the third stage were analysed for total heavy mineral (THM) and a magnetic fractionation was conducted using a Carpco lift magnet. NM $TiO_2$ and NM zircon were determined by XRF analysis.

The conductor product (rutile) was 50.6% $TiO_2$ with 9.8% zircon. The non-conductor product (zircon) was 2.7% $TiO_2$ and 70.5% zircon. The NM content of the feed was 80.3%, which ties in with the 86.5% combined conductor and non-conductor mass yield. The NM content increased from 89.9% to 98.1% for the conductor product after RER separation, whereas the NM content increased from 77.3% to 95.2% for the non-conductor product. The $TiO_2$ and zircon grades for

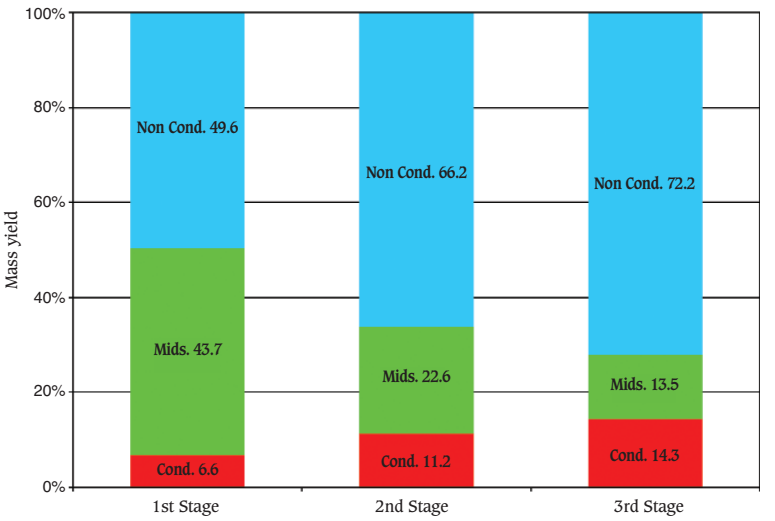


**Figure 14—Typical variation of mass yield for HTR**

the RER products are noted for this feed in Table IV. The mass yields to non-mags for both conductor and non-conductor RER separation was 79% and 73% respectively after three stages with the non-magnetic fraction retreated.

### *Dry magnetic separation*

RER magnetic separation tests were conducted using a three-stage non-magnetic retreat configuration on both the conductor and non-conductor products. The roll speed was reduced for each subsequent stage. The 150 mm diameter roll was fed via a hopper and vibratory feeder. The feed rate was calculated to be 3.0 TPH/m. Preliminary tests were conducted on 3:1 and 4:2 (magnet: steel) spacing configurations of the roll. The magnetic and mids fractions were combined as tailings. The splitter was adjusted during the tests to just touch the curve of non-magnetic material as it was released from the roll.

In Table IV the analysis and yields relate to the performance of the RER on the conductors and non-conductors of the HTR. The recovery is based on the feed to the HTR. The non-mags from the conductor treatment would be fed to the rutile circuit at the mineral separation plant. The non-mags from the non-conductor treatment would enter the zircon circuit. Similar grades of $TiO_2$ were produced in previous tests, so quality is maintained for different feed types. The non-mags mass yield gives an indication of the high NM grade in the rutile-rich feed.

MLA analysis received for the mags from the RER test work reveal that the non-conductor mags contained 26.8% epidotes, 29.6% zircon and 28.9% pyroxene. The conductor mags contained 6.6% epidotes, 13.9% leucoxene, 50.1% rutile and 6.9% zircon.

*Table IV*

**RER performance on rutile and zircon product grade and recovery**

| | Mass yield % | | N/mags | | | |
|---|---|---|---|---|---|---|
| | Mags | N/mags | $TiO_2$ | | Zircon | |
| | Grade% | Recovery% | Grade% | Recovery% | | |
| Conductor | 21.0 | 79.0 | 70.1 | 45.2 | 10.1 | 1.9 |
| Non-cond | 27.0 | 73.0 | 5.4 | 17.4 | 86.0 | 81.2 |

*Table V*

**Feed and products from bulk simulation on mixed feed**

| | Product stream | | | |
|---|---|---|---|---|
| | Feed% | Ilmenite% | Zircon% | Rutile% |
| Amphibole | 7.29 | 0.62 | 0.02 | 0.00 |
| Chromite | 0.97 | 1.89 | 0.00 | 0.00 |
| Epidote | 12.10 | 0.33 | 1.10 | 0.19 |
| Feldspar | 0.56 | 0.09 | 0.05 | 0.03 |
| Garnet | 5.24 | 3.96 | 0.43 | 0.04 |
| Haematite | 2.05 | 3.21 | 1.61 | 0.48 |
| Ilmenite | 13.45 | 69.95 | 0.02 | 0.12 |
| Ilmenite-Alt | 1.27 | 2.92 | 0.00 | 0.10 |
| Leucoxene | 1.85 | 0.81 | 0.65 | 8.77 |
| Magnetite | 2.86 | 9.43 | 0.00 | 0.02 |
| Other | 0.34 | 0.10 | 0.03 | 0.67 |
| Pyroxene | 11.50 | 0.54 | 1.88 | 0.06 |
| Quartz | 13.03 | 0.24 | 0.36 | 0.79 |
| Rutile | 5.47 | 0.76 | 3.32 | 78.12 |
| Titanite-sphene | 0.48 | 0.10 | 0.97 | 0.70 |
| Tourmaline | 0.14 | 0.00 | 0.00 | 0.00 |
| Zircon | 14.45 | 0.14 | 88.58 | 9.66 |

## Conclusion

The mass yields for each stage of the bulk simulation were calculated from the tests done and, using the physical analysis grades of the intermediate products, the resulting recoveries over the complete circuit were calculated. The calculated recovery of the total valuable minerals from the feed is 56% for ilmenite, 34% rutile and 77% zircon.

Table V shows the MLA results received on the feed to the full circuit (MSP tails) and the subsequent analysis for the products of the test work. The amphibole, feldspar, tourmaline, epidotes and pyroxene from the feed stream were rejected over the whole process in the Floatex overflow, spiral tails, WREDMS and WHIMS tails, HTR mids and RER mags.

The partial analysis (Table V) confirms the mass balance grade and recoveries calculated for the test work conducted. A more detailed analysis than the magnetic fractionation gives a better indication of the minerals present in the products from the bulk simulation. Magnetite, garnet, haematite and chromite are concentrated in the ilmenite product. Ilmenite grade is increased over five times from the feed to the process. Altered ilmenite accounts for nearly 3% of this product for the mixed feed type. Rutile, pyroxene, haematite and epidotes contaminate the zircon-rich product. The rutile-rich product is approximately 9% leucoxene and 10% zircon. Images produced by MLA will also give a better representation of inclusions that may be present in the products.

Using the method of bulk simulation in the pilot plant, the mass balance with associated grades and recoveries has been confirmed for combined stockpiled and current MSP tailings. The products from the dry circuit are of suitable quality to supplement the feed to the dry mills at the Mineral Separation Plant. The non-magnetic minerals would undergo electrostatic before magnetic separation. Further bulk simulations can be used to determine the variation of product grade with variation in head feed. The addition of WREDMS in the process and efficient operation of the WHIMS are critical for keeping the smelter feed ilmenite product within the required impurity specifications.

The correlation between the physical analysis and MLA gives a fine indication of the reliability of the bulk simulation method. Good operational and process equipment knowledge can ensure that the results are reproducible on a larger scale if the attention to basic principles is maintained.

## References


1. Wightman, E. Mineralogical Characterisation of RBM Tails Samples, Unpublished report, June 2005.
2. Outokumpu Technology, Physical Characteristics of Select Minerals and Materials, May 2006.
3. Holland-Batt, A.B. Analysis of Mineral Separation Systems by means of Recovery Functions, *Trans. Instn. Min. Metall.* vol. 94, March 1985. pp. C17–C29. ◆